Title: Identification of Peptidoglycan Recognition Protein 3 coated microbes in subgingival dental plaque in Periodontitis

Running title: Identify PGRP3 coated plaque microbes in periodontitis

Authors: Jing I. Yang[*], Justin Merritt † ‡, Jens Kreth[2], Sukirth Ganesan§, Shareef M. Dabdoub ‖, Li-Jung Lin¶, Sivaraman Prakasam § †

*Advanced Education in Periodontics, Division of Periodontics, Department of Regenerative and Reconstructive Sciences, School of Dentistry, Oregon Health and Science University, Portland, Oregon
† Division of Biomaterials and Biomedical Sciences, Department of Oral Rehabilitation and Biosciences, School of Dentistry, Oregon Health and Science University, Portland, Oregon
‡ Department of Molecular Microbiology and Immunology, School of Medicine, Oregon Health and Science University, Portland, Oregon
§ Department of Periodontology, College of Dentistry and Dental Clinic, the University of Iowa, Iowa city, Iowa
‖ Division of Biostatistics and Computational Biology, College of Dentistry and Dental Clinic, the University of Iowa, Iowa city, Iowa
¶ Division of Periodontics, Department of Regenerative and Reconstructive Sciences, School of Dentistry, Oregon Health and Science University, Portland, Oregon

Acknowledgments:
This study was fully funded by NIDCR/NIH (DE031013).
Jim A. Katancik; Department of Regenerative and Reconstructive Sciences, School of Dentistry, Oregon Health and Science University, Portland, Oregon
Phillip T. Marucha; Division of Periodontics, Department of Regenerative and Reconstructive Sciences, School of Dentistry, Oregon Health and Science University, Portland, Oregon

Conflict of Interest: None of authors reported any conflict of interest

Summary*: Peptidoglycan Recognition Protein 3 (PGRP3) highly coated microbes are shown in higher relative abundance in periodontitis subgingival microbial plaque.*

Total Word Count: 4627 words
Number of figures: 10
Number of tables: 2
Number of references: 48

Abstract

Background: Peptidoglycan recognition protein 3 (PGRP3), a pattern recognition receptor (PRR) is known to promote a homeostatic environment by maintaining a symbiotic microbiome. These secreted PRRs act by binding to different microbial-associated molecular patterns and presumably coat microbes. However, the specificity of binding/coating at the microbial species level is unknown. We have used the coating ability of PGPR3 to isolate in vivo PGRP3 coated microbes from subgingival dental plaque of stage III/IV periodontitis subjects. We have further identified PGRP3 highly coated species versus non-coated species in the isolated samples using 16S rRNA sequencing.

Methods:12 participants including 8 periodontitis subjects and 4 non-periodontitis subjects participated in the study. Clinical periodontal data was collected for all subjects and microbial dental plaque samples were collected from the subgingival pockets prior to periodontal therapy. PGRP3 highly coated bacteria were separated from non-coated bacteria using two steps of antibody assisted separation; magnetic activated flow cell sorting (MACS) followed by fluorescence activated cell sorting (FACS). Sorted samples were analyzed via 16S sequencing to characterize the microbiome of each sorted fraction.

Results: All clinical parameters were significantly different between the periodontitis and non-periodontitis groups including probing depth (PD), bleeding on probing (BOP), plaque index, and radiographic bone loss. There were significantly higher numbers of PGRP3 coated bacteria in periodontitis subjects compared to minimal to no PGRP3 coated bacteria in non-periodontitis subjects. Sorted fractions had significant beta diversity. Top PGRP3 coated bacteria identified include *Porphyromonas gingivalis, Corynebacterium durum, Streptococcus mutans,* and *Neisseria. Sp*.

Conclusion: PGRP3 coated bacteria are abundant during periodontitis. PGRP3 coated bacteria include putative periodontal pathogens, opportunistic pathogens, and commensals, suggesting context specific functions for PGRP3 coating. PGRP3 coating may also be species specific as evidenced by differential coating with three different species of *Treponema*.

Keywords

Periodontitis; cross sectional; dental plaque/dental microbial biofilm; peptidoglycan recognition protein; pattern recognition protein; innate immunity; host response

Plain text summary: PGRP3 is a protein that helps the body recognize and respond to bacteria based on the essential structures of the bacteria. They are believed to act by helping to maintain a beneficial microbial community. These proteins can attach to bacteria and coat them. However, it is unknown which bacteria they bind to. Here we separated the PGRP3 coated bacteria from dental plaque samples collected from individuals with severe periodontitis and individuals who did not have a diagnosis of periodontitis (non-periodontitis). We used an antibody-based separation technique to purify PGRP3 coated bacteria to a high level of purity. We then sequenced the DNA of the separated bacteria to identify species. We found that samples obtained from non-periodontitis subjects did not have enough PGRP3 coated bacteria to allow for purification. However, the periodontitis samples had significant numbers of PGRP3 coated bacteria. We also identified the following species as PGRP3 highly coated, i.e., Porphyromonas gingivalis, Corynebacterium durum, Streptococcus mutans, and Neisseria. Sp. Species that are not coated with PGRP3 include the following, Leptotrichia wadei, Selenomonas artemidis, Prevotella salivae, and Leptotrichia shahii. While it appears that PGRP3 coats putative oral pathogens including Porphyromonas gingivalis and Streptococcus mutans, PGRP3 coating specificity is noted in only one of the three Treponema species, suggesting a species-level specificity of PGRP3 binding.

Introduction

Periodontitis is a dysbiotic inflammatory disease that is initiated by dental plaque and results in the inflammatory destruction of the periodontium. The inflammatory destruction in turn disrupts the homeostatic balance between resident microbiota and the host, which further promotes progression of inflammation and destruction of the periodontal apparatus [1 2 3 4]. Innate immunity serves as the first line of defense in host immune response and has long been investigated in the context of periodontitis. Pattern recognition receptors like Peptidoglycan recognition proteins (PGRPs) are key components of the innate immune system and play an important role in maintaining the homeostatic balance between the host and tissue residing microbes.

PGRPs are highly conserved through the evolutionary tree[5]. The four known human isoforms of PGRP, namely PGRP1 through PGRP4, are secreted proteins. PGRP3 and PGRP4 are chiefly expressed by epithelial cells at mucosal surfaces, presumably to facilitate host-microbe interactions. While all four PGRP isoforms have been implicated in chronic inflammatory diseases in knock out mice models, PGRP3 in particular is the least studied [6 7 8 9]. PGRP3 has been proposed to be a critical player in chronic inflammatory diseases including atopic dermatitis, ulcerative colitis, and other dysbiotic inflammatory diseases. PGRP3 has been characterized as both antimicrobial and anti-inflammatory [6].

PGRP3 and PGPR4 genes are located in close proximity to the *PSORS4* gene, a susceptibility gene for psoriasis located within the epidermal-differentiation-complex gene cluster on chromosome 1q21, a region containing a susceptibility gene(s) (*PSORS4*) for psoriasis[9]. Tonsillar epithelial cells release PGRP3 and PGRP4 in response to recognition of peptidoglycan via another PRR group namely, toll like receptors (TLR)[9]. In an *in vivo* mouse experimental dermatitis model, the absence of PGRP3 expression has been shown to cause to more severe oxazolone induced dermatitis [10]. Higher serum levels of PGRP3 are also associated with greater reduction of pro-inflammatory cytokines including interleukin-4, interferon gamma, and tumor necrotic factor-alpha[11]. Furthermore, a deficiency of PGRP3 can induce colitis in mice, leading to ulcerations, hyperplasia, and loss of epithelium in colonic mucosa[12]. A PGRP3 knock out also displays a dysbiotic gut microflora. In summary, in mouse models it has been established that PGRP3 is crucial for maintaining microbial homeostasis on mucosal surfaces and its absence or reduction results in dysbiosis of the tissue microbiome.

In contrast to the anti-inflammatory effect of PGRP3 in mouse models, *in vitro* experiments with mammalian cells show that this protein elicits a pro-inflammatory response by selectively binding to microbes and enhancing macrophage phagocytosis of *S. aureus* and peptidoglycan [13]. This suggests that PGRP3 might have a cell or stimuli dependent dual function. PGRP3 regulation in carcinomas further supports this concept of a divalent and contextual function of PGRP3 [14]. We have previously reported that PGRP3 is increased in saliva and the gingiva of periodontitis subjects compared to healthy controls. However, the consequence of upregulation remains poorly understood. Through *in vitro* experiments we have also demonstrated that PGRP3 selectively binds putative periodontal pathogens. Based on these observations we hypothesized that PGRP3 may specifically target certain microbial strains through binding or 'coating' of these microbes in subgingival dental biofilm in periodontitis. Here, we take advantage of the ability of PGRP3 to coat bacteria to isolate PGRP3 coated microbes to a high level of purity by adapting a previously described two step antibody aided microbial sorting

technique; magnetic activated cell sorting (MACS) [15] followed by fluorescence activated cell sorting (FACS) [16]. The sorted microbial plaque fractions were analyzed with 16S rRNA microbial sequencing and the microbial species that were overrepresented in the different sorted fraction were identified.

Material and Methods

Study Population

The Institutional Review Board of the Oregon Health and Science University (OHSU IRB) approved the study (STUDY00023024). The study was conducted in accordance with the standards outlined in the Declaration of Helsinki. Subjects between the ages of 18 and 80 were recruited from the OHSU School of Dentistry (SOD). Inclusion criteria included, subjects categorized as ASA I or II. Exclusion criteria included subjects who actively use tobacco or recreational drugs, who were pregnant, currently breastfeeding, who had periodontal therapy in the past 6 months, and have active infectious disease or any mental disability that would affect compliance/consent. Complete clinical and radiographic examinations were performed by two investigators (S.P and J.Y.) Complete periodontal charting data was recorded including probing depth, clinical attachment level, modified O' Leary plaque index [17], bleeding on probing, mobility [18], furcation involvement [19]. Radiographic bone loss was evaluated through a complete mouth series of radiographs. The periodontitis group (PD) included generalized periodontitis stage III or stage IV, grade B or grade C, as per the 2017 World Workshop Classification [20]. The non-periodontitis group (HG) served as controls and include subjects diagnosed with periodontal health or dental plaque induced gingivitis on an intact periodontium[21].

Plaque sample collection

Plaque collection was done in strict accordance with the NIH Human Microbiome project's Core Microbiome Sampling Protocol A (HMP-A)[22]. After evaluation, subjects from both groups were instructed to not perform oral hygiene on the morning of the sample collection appointment. Subjects rinsed their mouth with water prior to sample collection. After isolation of the area with cotton rolls, supra and marginal plaque was removed, and the plaque sample was collected from the mesio-buccal surface of the selected teeth from sites with probing depth 6 mm using a sterile mini Gracey curette. The curette tip was immersed in phosphate buffered saline (PBS), for 4-5 seconds with gentle shaking. The face of the curette was then wiped on the inside edge of the collection tube. Samples collected from all teeth were pooled. Samples were transported immediately in ice to the lab for further processing.

Separation of highly coated PGRP3 microbes via two-step sorting Magnetic Activated cell Sorting (MACS) followed by Fluorescence activated Cell Sorting (FACS):

Samples were homogenized and centrifuged (50g, 15 min, 4°C) to remove large particle debris. The bacteria-containing supernatants were removed (100µl/sample), washed with 1 ml of PBS containing 1% (w/v) bovine serum albumin (staining buffer, SB) and centrifuged for 5 min (8,000g, 4°C) before resuspension in 0.5ml SB. 20µl of this suspension was saved as the pre-sort sample for 16S sequencing. After an additional wash, pellets were resuspended in 100µl blocking buffer (SB containing 20% normal mouse serum), incubated for 20 m on ice, and then stained with 100 µl SB containing FITC-conjugated anti-human PGRP3 antibody (10µg/µl) [23] for 30 min on ice. Samples then were washed thrice with 1ml SB before flow analysis or cell separation. Anti-human PGRP3 stained plaque bacteria were incubated in 1ml SB containing 50µl anti-FITC

MACS beads (15 min at 4°C) [15], washed twice with 1ml SB (10,000xg, 5 min, 4°C), and then sorted by MACS. After MACS separation, 50 µl of the negative flow-through fraction was collected for later 16S sequencing. The positive fraction was then further purified via FACS and collected, quantified, pelleted (10,000g, 5 min, 4°C), and then stored at −80°C with the pre-sort and PGRP3- bacteria samples.

16S rRNA Sequencing and Microbiome Analysis

Frozen Pellets collected from the presorted fraction, magnetic negative fraction, magnetic positive fluorescence negative fraction, and fluorescence positive fraction, were thawed and transferred to PCR tubes in preparation for DNA extraction. PCR tubes were centrifuged at 8,000 RPM for one minute. 180 µl of ATL and 40 µl of proteinase K were allotted to each sample[24-26]. Samples were vortexed for 15 seconds and then incubated in a dry water bath at 56°C overnight. The second day, 200 µl of Buffer AL[25] was allocated to each tube and then mixed for 15 seconds. Samples were placed in a dry water bath again at 70°C for 10 minutes. 200 µl of 100% EtOH was placed in each sample, then vortexed for 15 seconds. This solution was transferred to a combined spin column/collection tube and centrifuged at 8,000 RPM for one minute. The spin column was transferred to a new 2 ml collection tube, and 500 µl of buffer AW1[25,26] was added, and centrifuged at 8,000 RPM for one minute. 500 µl of buffer AW2 [25,26]was added and centrifuged at 14,000 RPM for 3 minutes. The collection tube was emptied of the solution and placed back in the centrifuge this time at 14,000 RPM for one minute. The solution in the collection tube was discarded and 50 µl of AE buffer[25] (preheated to 70°C) was added in each tube and incubated at room temperature for 5 minutes[26]. The tubes were placed for a final time in the centrifuge at 8,000 RPM for 1 minute and the spin columns with solution were stored in a freezer at -20°C until they were sent for further analysis[26].

Bioinformatics and statistical analysis.

Bioinformatics analysis was done by a biostatistician (S.D). Extracted bacterial DNA samples were quantified using Qubit and the quality was verified using gel electrophoresis. After normalization, the V3-V4 regions of the 16S rRNA gene were amplified in the Illumina MiSeq (2*300bp PE) platform according to the Illumina protocol [27] [28] at the University of Iowa Microbiome Core. 16S rRNA data analysis was conducted using R-based Divisive Amplicon Denoising Algorithm-2 (DADA2) [29], and Quantitative Insights into Microbial Ecology (QIIME2) [30]. DADA2 utilizes amplicon sequence variant (ASV)- based analysis instead of operational taxonomic unit (OTU) assignments based on the commonly used 97% similarity. ASVs were assigned a taxonomic identity using the naïve-Bays algorithm implemented in QIIME2 [31] and trained on the Human Oral Microbiome Database (HOMD) v9.15 [32]. Alpha diversity (within groups) was assessed with the Abundance Coverage Estimator (ACE). Beta diversity (between groups) was estimated using partial least squares-discriminant analysis (PLS-DA) [33]. Principal Coordinate Analysis (PCoA) and Linear Discriminant Analysis were performed on variance-stabilized relative abundances of species-level ASVs. The significance of clustering was determined using the PERMANOVA test of the difference in clustering centroids. Significantly different species between the four groups were determined using MaAslin2 of R package [34]. Results were visualized using PhyloToAST [35]. For each environment, species identified in at least 80% of the subjects were identified using QIIME's core_microbiome.py script.

Results

Study population

Twelve subjects were recruited from the OHSU SOD after screening. Characteristics of the periodontitis group (PD, n=8) and non-periodontitis group (HG, n=4) are listed in Table 1. The average age of the study population was 50 years old, (HG = 50 and PD = 50; P=0.49, NS). Among the subjects, 58% were male and 42% were female (P=0.14). Most of the subjects self-reported as Caucasians (77%). Asian and Hispanic constituted the "other" ethnicity groups (Table 1), 8% and 15%, respectively. All subjects fell under the category of ASA I or ASA II. The periodontal status of the subjects, including clinical findings and diagnosis are summarized in Table 1. In the HG group, 25% of patients demonstrated periodontal health, with 75% of them presenting gingivitis; in PD group, all patients (100%) had periodontitis. In the PD group, all the subjects presented with gingival inflammation (100%); 6 subjects were diagnosed with periodontitis stage III grade B (75%), and 2 subjects were diagnosed with stage IV grade C (25%). In the HG group, the range of probing depths was 1 to 6mm), with an average probing depth of 2.4mm; in PD group, the range of probing depths was 1 to 12mm, with the average probing depth of 3.9mm. The difference between the average probing depth between HG and PD group was statistically significant (difference= 1.5mm, $P<0.05$). The average radiographic bone loss at the most severe site was averaged 2.5% and 35% respectively for the HG and PD groups ($P<0.05$, Table 1). In the HG group, bleeding on probing index was 6%; whereas in PD group, the bleeding index was 61%, and the difference between two groups was significant ($P<0.05$). The plaque index in the HG group was 34%, and in PD group it is 94% ($P<0.05$).

Flow Cytometry Results

Of the 12 subjects, six PD plaque samples and three HG samples were successfully processed and analyzed via flow cytometry. All the samples acquired and processed showed significant differences between the HG and PD groups regarding the total number and percentage of microbes that are PGRP3 coated (Figure 1-4). FACS purification was done on the MACS positive flow fraction. FACS purification gating was set stringently to ensure high levels of coating as shown in Figure 1 for the HG and Figure 2 for the PD group. Unstained samples and isotype labelled samples were used to help set the appropriate gating. Gating was done at the highest FITC fluorescence intensity range to collect the PGRP3+ fraction. Lower ranges were used to collect the PGRP3-ve fraction. Midrange fluorescence intensities that overlapped with isotype staining were discarded (Figures 1c and 2c, selection area of FITC- and FITC+ area).

FACS analysis revealed a significantly higher proportion of PGRP3 coated microbes in the PD group. The HG group, after MACS sorting, had virtually no PGRP3 coated microbes based on the stringent gating strategy used (Figure 2, purple, 0.1% FITC positive). Most of the microbes in this fraction were PGRP3 negative (Figure 1, red, FITC negative, 97.6%). The PD samples showed a significantly higher composition of PGRP3 coated microbes (Figure 2, purple, FITC positive, 94.9%).

The abundance of cells sorted by fluorescence intensity was compared between the positive and negative controls in the HG and PD groups (Figures 3 and 4). In the HG MACS positive FITC positive fraction, most cells had low fluorescence intensity, suggesting that the microbes in the fraction were coated with PGRP3 (Figure 3a). However, in PD group, this double positive fraction had a higher abundance of cells with high fluorescence intensity (Figure 4a).

MACS negative sort fractions tested under FACS had an absence of PGRP3 coated bacteria in both the HG and PD groups (Figure 3b, 4b). MACS positive and FITC negative sort fractions had low mean fluorescent intensity (Figure 3c, 4c). IgG isotype controls were used to test the non-specific binding of FITC to the microbes, which also showed low mean fluorescent intensity in FACS (Figure 3d, 4d). The unstained pre-sort fraction served as a negative control (Figure 3e, 4e). The unstained and isotype control samples were used to set gating for sorting by FACS. Table 2 summarizes the flow cytometry data for all nine subject samples. The PD group (Table 2, P1-P6) showed a significantly higher abundance of PGRP3 positive single cells (FITC+) than the HG group (Table 2, H1-3). In addition, the percentage of PGRP3 positive microbes was significantly higher across the panel in the PD group than HG group (FITC+ % parent).

Microbial Analysis

DNA and genome study results were successfully obtained from eight PD samples. Taxonomic information was compared between the four groups, the presort fraction, MACS negative fraction, MACS positive and fluorescent negative fraction, and MACS positive fluorescence positive fraction. The alpha diversity in the samples was determined using the Abundance Coverage Estimator (ACE) metric [36] (Figure 5). ACE accounts for both species richness and abundance values. There is no significant difference between the four groups in terms of alpha diversity (Figure 5, x-axis).

Beta-diversity was determined by the partial least squares-discriminant analysis (PLS-DA) (Figure 6). This estimated and maximized the dissimilarity of the species composition between all four groups. Each dot on the graph signified the cluster of one plaque sample with two metrics on PLS-DA. The distance between the two dots on the map indicated the relevant difference in species composition and diversity between the two groups. Principal Coordinate Analysis (PCoA) and Linear Discriminant Analysis were performed on variance-stabilized relative abundances of species-level ASVs (Figure 6). The Presort group (Figure 6, green) and fluorescence negative group (Figure 6, gray) showed distinct clustering patterns compared to either magnetic negative (Figure 6, gray) or fluorescence positive group (Figure 6, orange) with strong separation on the graph (PERMANOVA, P=0.001). The fluorescence positive group (Figure 6, orange) showed very limited overlap between the presort group (Figure 6, green) or fluorescence negative group (Figure 6, gray). This distinction marked the difference in species composition between fluorescence positive and other groups, suggesting that the PGRP3 highly coated microbial group was significantly different in species diversity.

The relative abundance of different species was compared between the presort group and other groups, including magnetic positive, fluorescence positive, and fluorescence negative groups (Figure 7). Results are shown as a heat map listing the top 50 microbial species in dental biofilm, using QIIME's core_microbiome.py script. Relative abundance differences were mapped as either positive (Figure 7, red) or negative (blue), on the gradient scale. *Porphyromonas. gingivalis*, for instance, had a significantly increased relative abundance in the fluorescence positive group (red) and fluorescence negative group (red), but also a significantly decreased relative abundance in the magnetic negative group (blue). Similar color patterns were also noted in the microbial species *Corynebacterium. durum, Neisseria. Sp., Actinomycetes. Sp., Bacteroidetes, Gracillibacteria*. On the other hand, select microbial species have higher

abundance in magnetic negative and presort, compared to fluorescence positive group. This group includes *Leptotrichia. shahii, Saccharibacteria Sp., Prevotella Sp.,* and *Treponema. Sp* (Figure 7).

The relative abundances of selected microbial species are shown in Figures 8 to 14. Relative abundance is shown as four column bars for four groups: presort, fluorescence positive, fluorescence negative, and magnetic negative group. In Figure 8, six microbial species are shown as selected examples of PGRP3 highly coated microbes, including *P. gingivalis, Corynebacterium durum, Neisseria sp., Streptococcus mutans, Lawsonella clevelandenesis, and unknown Enterobacteriaces.* Those microbial species all showed higher abundance in the MACS fluorescence double positive group than the presort fraction and MACS negative group (Figure 8). *P. gingivalis* showed the highest relative quantity of cell counts among all other species (Figure 8, 5000-10000).

In contrast, four microbial species are shown in Figure 9 as examples of bacteria that are not coated with PGRP3. Those were *Leptotrichia wadei, Selenomonas. Artemidis, Prevotella salivae, Leptotrichia. Shahii.* Those species all showed lower abundance in the fluorescence positive group than the presort and magnetic negative group (Figure 9). To illustrate that PGRP3 coating differences can occur at species level we have shown the data from three different strains of *Treponema. sp* in Figure 10. Two strains, *Treponema.sp*._HMT_262 (Figure 10, top left) and *Treponema.sp*._HMT_927 (Figure 10, top right) showed higher relative abundance in presort (Figure 10, blue) and magnetic negative group (Figure 10, green) than fluorescence groups suggesting these species are not coated with PGRP3. However, *Treponema.sp*._HMT_257 (Figure 10, bottom left), appears to be highly coated with PGRP3 with higher relative abundance compared to the other sort fractions.

Discussion

Human PGRP3, part of the PGRP family of pattern recognition receptors, extends the innate immune defense as a secreted and soluble protein [37 38]. In addition, PGRPs are unique host-microbiome mediators as they may be antimicrobial and have host modulatory functions [37 38]. PGRP3 is thus emerging as one of the crucial mediators of mucosal homeostasis[39]. For example in mice PGRP3 knockout results in a dysbiotic microbiome and dysregulation of T cell mediated immunity[39]. However, the role of PGRP3 in periodontitis remains poorly understood.

We have previously reported that elevated levels of PGRP3 can be detected in the supernatant of unstimulated whole saliva of individuals with periodontitis compared to healthy subjects [40]. Interestingly, in these individuals we also detected PGRP3 bound to bacteria that are in the pelleted fraction (data not shown). Through in vitro binding assays we observed that PGRP3 shows higher affinity to test oral putative pathogen, *P. gingivalis* (Data not shown). Here we show that similar to saliva, PGRP3 coated bacteria can be detected in subgingival dental biofilm. However, PGRP3 coated bacteria are detected only in subgingival plaque of periodontitis subjects and not in health or gingivitis subgingival plaque samples.

In our study, PGRP3 expression is much lower in health and gingivitis compared to periodontitis. This combined with the fact that there are much lower amounts of subgingival/crevicular plaque in health/gingivitis could explain the absence of detectable PGRP3 coated bacteria in non-

periodontitis samples. The percentage of PGRP3 coated bacteria in the periodontitis samples is also much lower compared to percentages detected in saliva [37,40]. This can be attributed to the fact that PGRP3 is secreted from all epithelial surfaces and hence availability is much higher in saliva to coat the planktonic bacteria in saliva [37].

In contrast, the PGRP3 source in subgingival plaque is the epithelial cells lining the pocket and possibly other immune cells that are infiltrating the inflamed pocket [37]. PGRP3 coating will depend on the temporal expression of PGRP3 during the biofilm formation. The complexity of the biofilm may limit the diffusion and coating of PGRP3 once the biofilm is established. Conversely, the coating could aid in biofilm formation. An additional potential explanation for the lower levels of detection of PGRP3 coated bacteria could be due to the two-step purification protocol used in this study. The MACS purification step presumably would isolate all PGRP3 coated bacteria, which could be an aggregate of bacteria that are bound to each other but are subsequently disaggregated at the end of the collection cycle. Loss of antibody binding of PGRP3, or PGRP3 binding to bacteria presumably could explain the loss of PGRP3 positivity after magnetic activated separation step. Finally, the stringent gating strategy set to eliminate any ambiguity in PGRP3 coated vs. non-coated bacteria amplifies the low detection rate of PGRP3 coated bacteria.

With our yield of PGRP3 coated bacteria (MACS and FITC double positive), due to the double purification and stringent gating strategy, we were able to isolate the bacteria that are highly coated with PGRP3. The isolation strategy is validated by the significant differences in beta diversity that were noted between the the16S rRNA identified bacteria that constituted different sorted fractions. We were thus able to identify the bacteria that are overrepresented in the PGRP3 coated sort fraction compared to the presort fraction and MACS negative fraction. The PGRP3 coated fraction includes putative pathogens like *Porphyromonas gingivalis & Streptococcus mutans* commensals like *Corynebacterium durum, Actinomycetes sp., Bacterioidetes, Gracillibacteria* and opportunistic species like *Neisseria. Sp.* The sort fraction that didn't have any PGRP3 coating included mostly commensal species like Leptotrichia *wadei, Selenomonas artemidis, Prevotella salivae, Leptotrichia shahii.*

A significant finding is the identification of *Porphyromonas gingivalis* in the PGRP3 coated sorted fraction. This validates our in vitro finding of recombinant PGRP3 coating *Porphyromonas gingivalis* through unbiased in vivo sampling from diseased sites. *Porphyromonas gingivalis* is part of the red complex bacteria described by Socransky, that are known to be associated with the development of periodontitis[41 1 42]. Other studies confirmed that *P. gingivalis* appears in much higher prevalence in periodontitis, as it accounts for 86% of subgingival plaque samples from subjects with chronic periodontitis [43]. Further exploring whether PGRP3 binding is to present this bacterium to the immune system or alternatively to remove it from the mucosal surface would be interesting. The detection of the PGRP3 coated *P. gingivalis* in subgingival plaque illustrates at the minimum the stochastic trapping of these bacteria in the subgingival pocket instead of being flushed out of the diseased area. This presumably could contribute to the chronicity of the disease process. The detection of other species, for example, *Neisseria. Sp.,* and *Corynebacterium durum*, has several likely explanations that need to be explored further.

Another intriguing observation from our results is the selectivity of PGRP3 binding at a species level. For example, three different species of *Treponema.sp*. are overrepresented in the different sorted fractions. *Treponema.sp*._HMT_262, and *Treponema.sp*._HMT_927, are overrepresented in the MACS-ve fraction, suggesting that these species are not coated by PGRP3. However, *Treponema.sp*._HMT_257 is overrepresented in the PGRP3 coated fraction.

Therefore, we propose two possible explanations to interpret our findings related to PGRP3 coated species in subgingival microbiome. First, our findings could imply that PGRP3 has a dichotomic role in maintaining the homeostasis between microbiota and the host. On one hand, PGRP3 coats periodontitis pathogens including *P. gingivalis* that could elicit a pro-inflammatory response in the host. This finding is consistent with previous literature on PGRP3 induced hyperinflammatory response through Toll Like Receptor-2 mediated pathways[9]. On the other hand, PGRP3 also binds to commensal microbes such as *Neisseria. sp* and *Corynebacterium.sp* that potentially aid in restoring the homeostasis of the microbial ecosystem within the host [44 45]. Previous research showed that in induced metabolic syndrome, PGRP3 improves the survival of commensal microbiota including *Actinobacteria*, and *Epsilonproteobacteria* in gut environment [46]. It suggests that PGRP3 provides host resistance to microbial dysbiosis through improved survival of commensal bacteria and reduced pathogenic strains.

The second hypothesis is that the PGRP3 highly coated species might only exist in higher abundance in periodontitis plaque. Only one out of three *Treponema* subspecies was identified as PGRP3 highly coated. *Treponoma* is believed to have multiple lineages that few *Treponoma* species could be attributed to periodontitis or gingivitis[47], while most of the *Treponema* are considered as commensal in gingival health. In addition, certain microbes might be shifted to be from commensal to pathogenic at hyper-inflammatory status. For instance, *Neisseria sp.* could be an "opportunistic pathogen" that provides transitory contaminant in subgingival biofilm during the dysbiosis process in periodontitis[48 49 50]. Data reported that *Neisseria sp.* in subgingival biofilm is associated with chronic and generalized aggressive periodontitis [49 50]. This result was coined by the previous idea of "non-specific theory" in periodontitis pathogenesis [51], as the change of composition of the microbiota, rather than single or few "pathogenic" species, is the etiology of periodontitis [51]. Therefore, the higher prevalence of virulent species including few *Treponoma* and opportunistic microbes at diseased status could contribute to specific PGRP3 affinity to those microbes that are not pathogenic at health.

The results we report should be interpreted within the following limitations. The study is of a pilot nature as our sample size is limited. Secondly, our inability to isolate or the non-availability of PGRP3 coated in the non-periodontitis samples limits our ability to compare the PGRP3 coated between disease versus healthy state. As we discussed earlier subgingival plaque availability in the non-periodontitis group is limited (Non periodontitis group average PI= 33.79%). Due to the demographic nature of the study site, the participants of the study constituted a predominantly homogeneous ethnic group (77% of the Caucasians) and may not be representative of the general periodontitis population[52]. According to NHANES data from 2009 to 2014, Caucasians have the lowest periodontitis prevalence compared to other Hispanic and non-Hispanic black groups[52].

Overall, this study was the first to identify and characterize the PGRP3 highly coated microbial taxa in human periodontitis. It provides valuable insights into understanding the differential affinity of PGRP3 to microbial species. Additionally, the techniques in the study can be useful for understanding *in vivo* specificity of various PRR to microbial species.

Conclusion

Peptidoglycan recognition protein 3 (PGRP3) highly coated microbes are in higher abundance in periodontitis subgingival dental plaque compared to non-periodontitis plaque samples. Through 16S RNA sequencing we report the distinctive taxonomic composition and diversity of microbial species between the PGRP3 coated microbial group and the PGRP3 uncoated/negative group. The relative abundance of PGRP3 coated microbial species was calculated and the top PGRP3 coated microbial species include *Porphyromonas. gingivalis, Corynbacterium.dunrum, Streptococcus mutans, Neisseria.sp, Actinomycetes.sp, Bacterioidetes,* and *Gracillibacteria.* The characterization of PGRP3 highly coated microbial species demonstrates the differential affinity of PGRP3 in subgingival microbial biofilm and it provides a theoretical foundation for the understanding of the role of PGRP3 in microbial dysbiosis and host response in periodontitis.

Figure 1: Representative example of Fluorescence activated cell sorting (FACS) of PGRP3 coated microbes isolated from sub-gingival plaque HG group via MACS.
Purple: FITC positive. Green: all singlet cells selected. 5a (upper left): all stained single cells florescence topography sorted by SSC-A (y axis) and florescence intensity (x axis). Red: FITC negative. 5b (upper right): all stained single cells florescence topography sorted by FSC width (y axis) and florescence intensity (x axis). 5c (middle): all stained single cells sorted by PGRP-3 antibody. FITC- selected area: single cells with none or limited florescence intensity (PGRP-3 antibody negative cells). FITC+ selected area: single cells with high florescence intensity (PGRP-3 antibody positive cells). 5d: (bottom) table listing number of cells and percentage of singlets on total cells, gated by florescence intensity. FITC+ cells: 8 cells, 0.1% of total cells. FITC- cells: 7,644 cells, 97.6% of total cells.

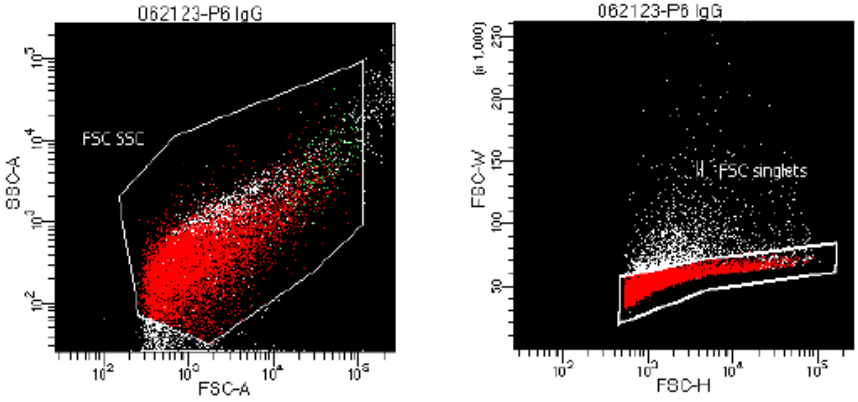

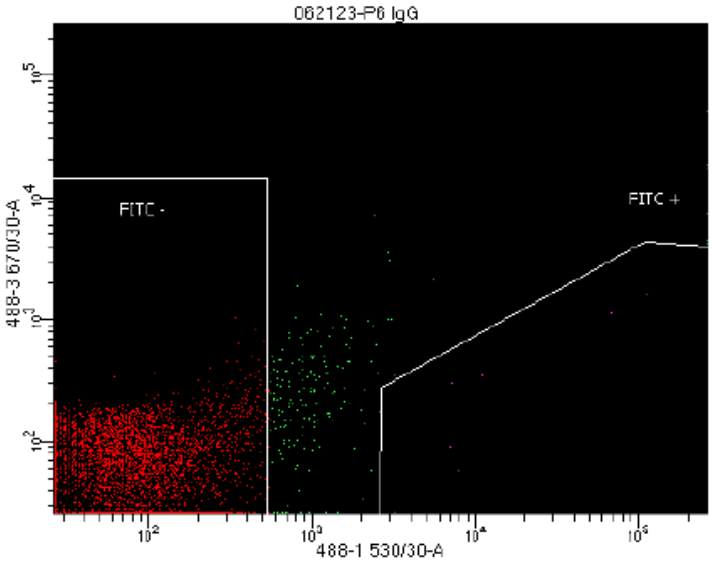

Tube: P6 IgG

Population	#Events	%Parent	%Total
All Events	10,000	####	100.0
FSC SSC	9,104	91.0	91.0
FSC singlets	7,831	86.0	78.3
FITC +	8	0.1	0.1
FITC -	7,644	97.6	76.4

Figure 2: Representative example of Fluorescence activated cell sorting (FACS) of PGRP3 coated microbes isolated from sub-gingival plaque PD group via MACS.
Purple/pink: FITC positive. Green: all single cells discarded to maintain stringency. Red: FITC negative.6a (upper left): all stained single cells florescence topography sorted by cell complexity SSC-A (y axis) and florescence intensity (x axis). 6b (upper right): cell florescence topography sorted by size -FSC width (y axis) and florescence intensity (x axis). 6c (middle): all cells sorted by PGRP-3 antibody. FITC- selected area (red): single cells with no FICS florescence intensity (PGRP-3 antibody negative cells). FITC+ selected area: single cells with high florescence intensity (PGRP-3 antibody positive cells). 6d: (bottom) table listing percentage of PGRP+ versus PGRP- using gating strategy. FITC+ cells: 6057 cells, 0.5% of total selected cells. FITC- cells: 1234803 cells, 94.9% of total selected cells.

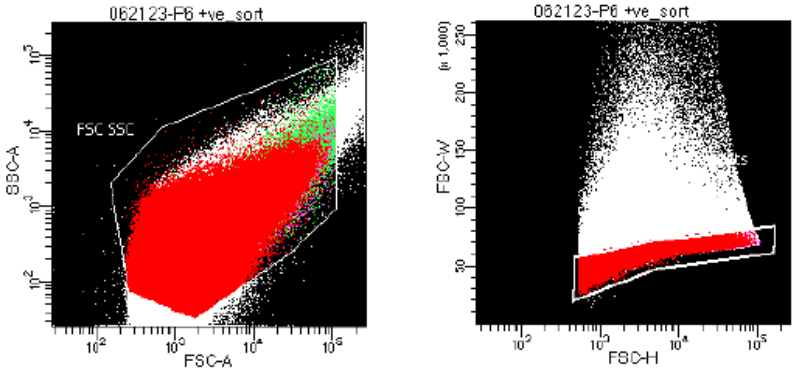

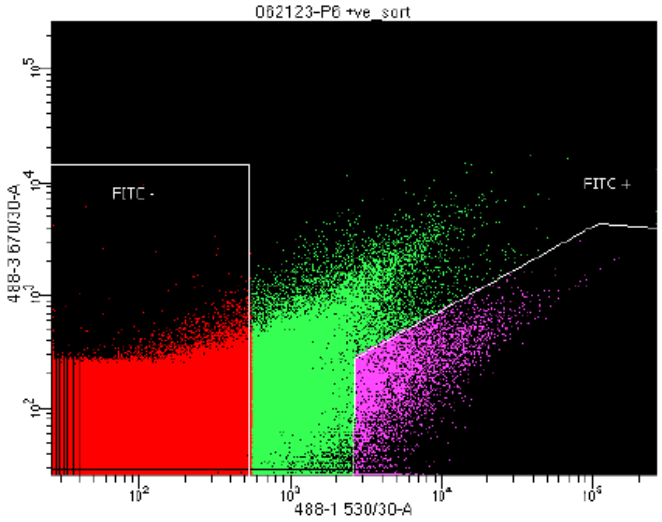

Tube: P6 +ve_sort

Population	#Events	%Parent	%Total
All Events	1,643,390	####	100.0
FSC SSC	1,566,158	95.3	95.3
FSC singlets	1,300,792	83.1	79.2
FITC +	6,057	0.5	0.4
FITC -	1,234,803	94.9	75.1

Figure 3: FACS analysis of different sort fractions from a non-periodontitis subject (HG). X axis: FACS fluorescence intensity. Y axis: number of cells counts. From left to right: 7a) PGRP3 positive fraction through MACS positive, PGRP3 antibody stained (FITCs) cell sample. 7b) MACS negative flow through portion, stained with FITC antibody. c) MACS positive FITC negative fraction. d) IgG isotype negative control. e) unstained negative control (presort fraction).

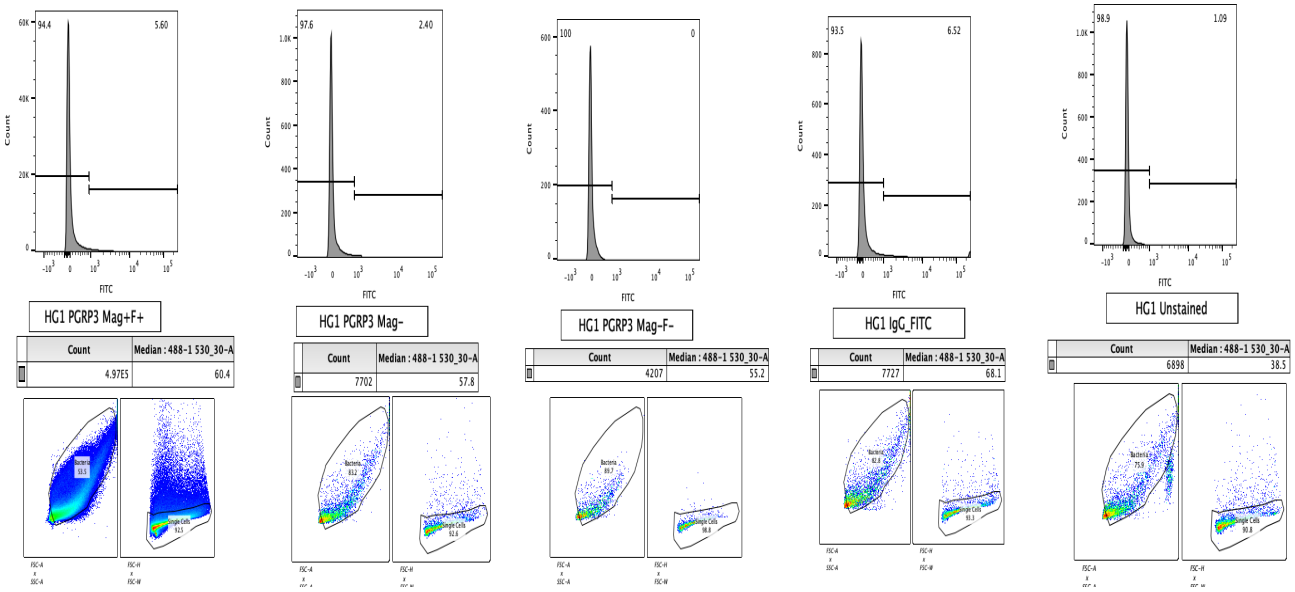

Figure 4: FACS analysis of different sort fractions from a periodontitis subject (PD).
From left to right: 1) PGRP3 positive fraction through MACS positive, PGRP3 antibody stained (FITCs) cell sample. 2) MACS negative flow through portion, stained with FITC antibody. 3) MACS positive FITC negative fraction. 4) IgG isotype negative control 5) (presort fraction).

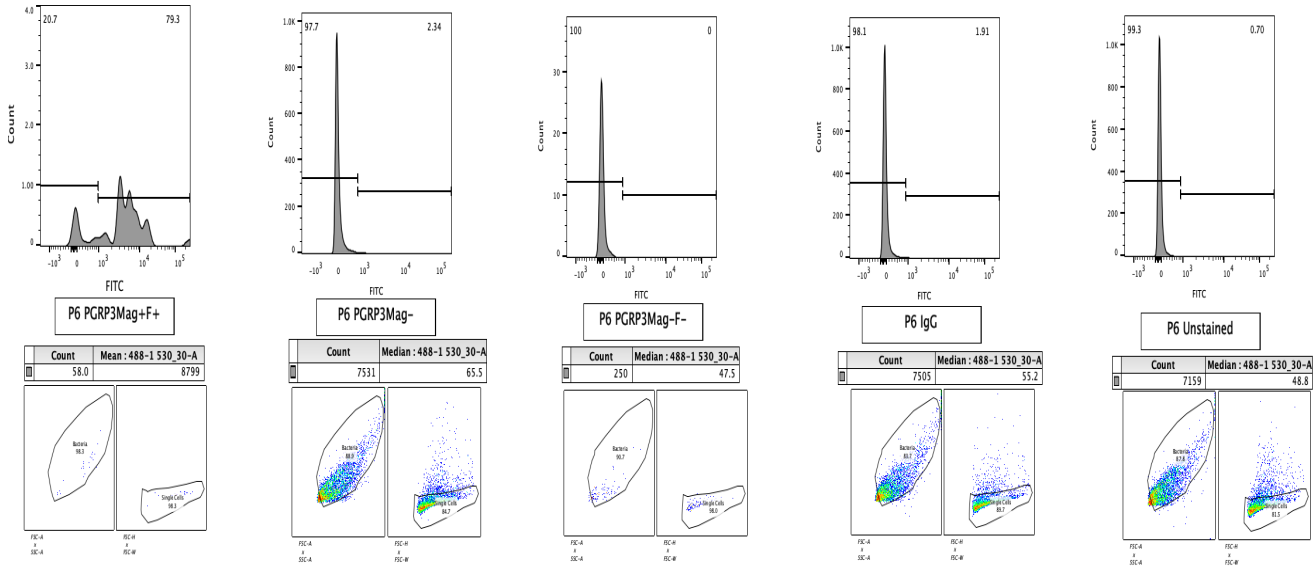

Figure 5: Alpha diversity determined by Abundance Coverage Estimator (ACE) metric

From top to bottom: Gray: presort fraction; Pink: PGRP3 fluorescence negative fraction; Purple: magnetic negative fraction control; Red: PGRP3 fluorescence positive fraction

X axis: species richness by ACE. All groups showed similar species richness in the range of 60-120, with slight difference in fluorescence negative fraction (pink). Y axis: Species density. Similar species densities were shown with peaks overlap between all groups.

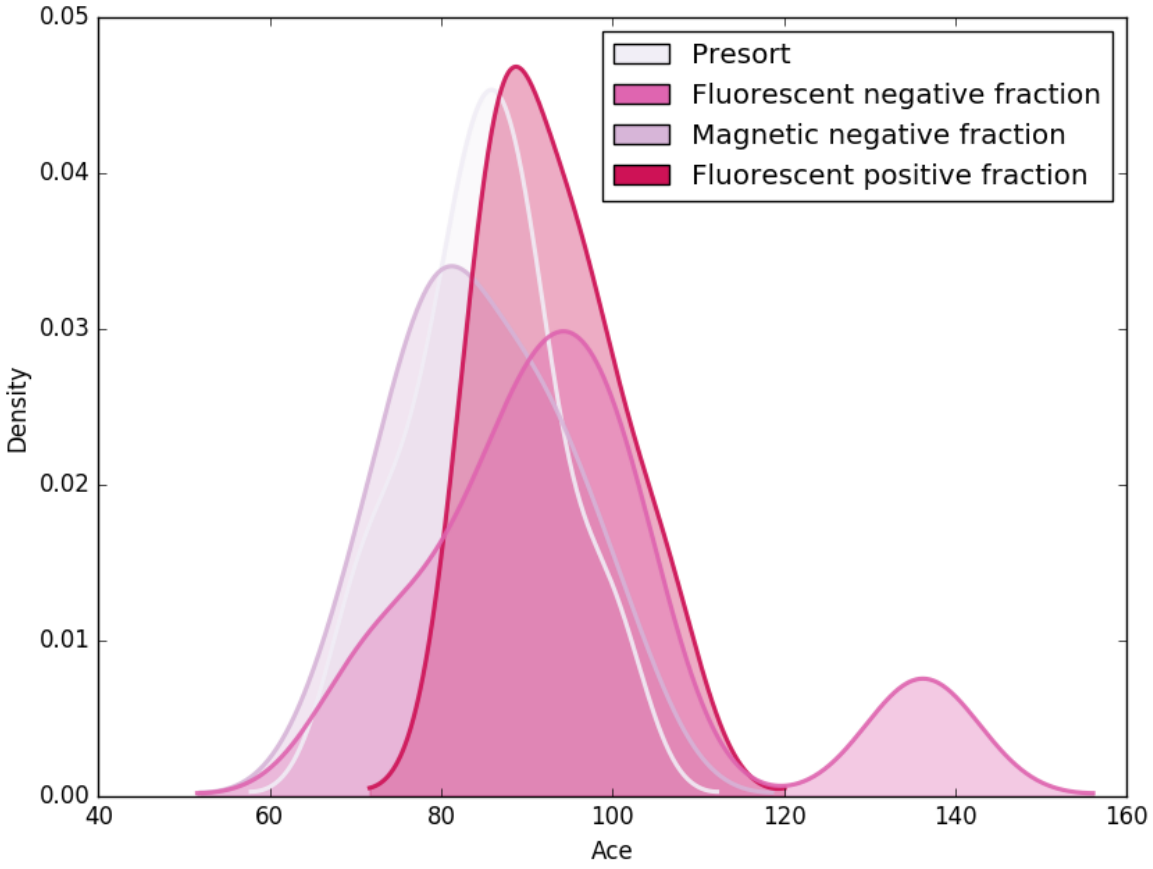

Figure 6. Beta diversity was determined by partial least squares-discriminant analysis (PLS-DA).
Four groups include presort group (green cross), magnetic negative fraction (gray plus), fluorescence positive fraction (orange triangle), and fluorescence negative fraction (blue circle). Significant clustering based on species composition (PERMANOVA, P=0.001) is evident between fluorescence positive and presort or fluorescence negative fraction, which suggests strong clustering of fluorescence group in relation to other groups.

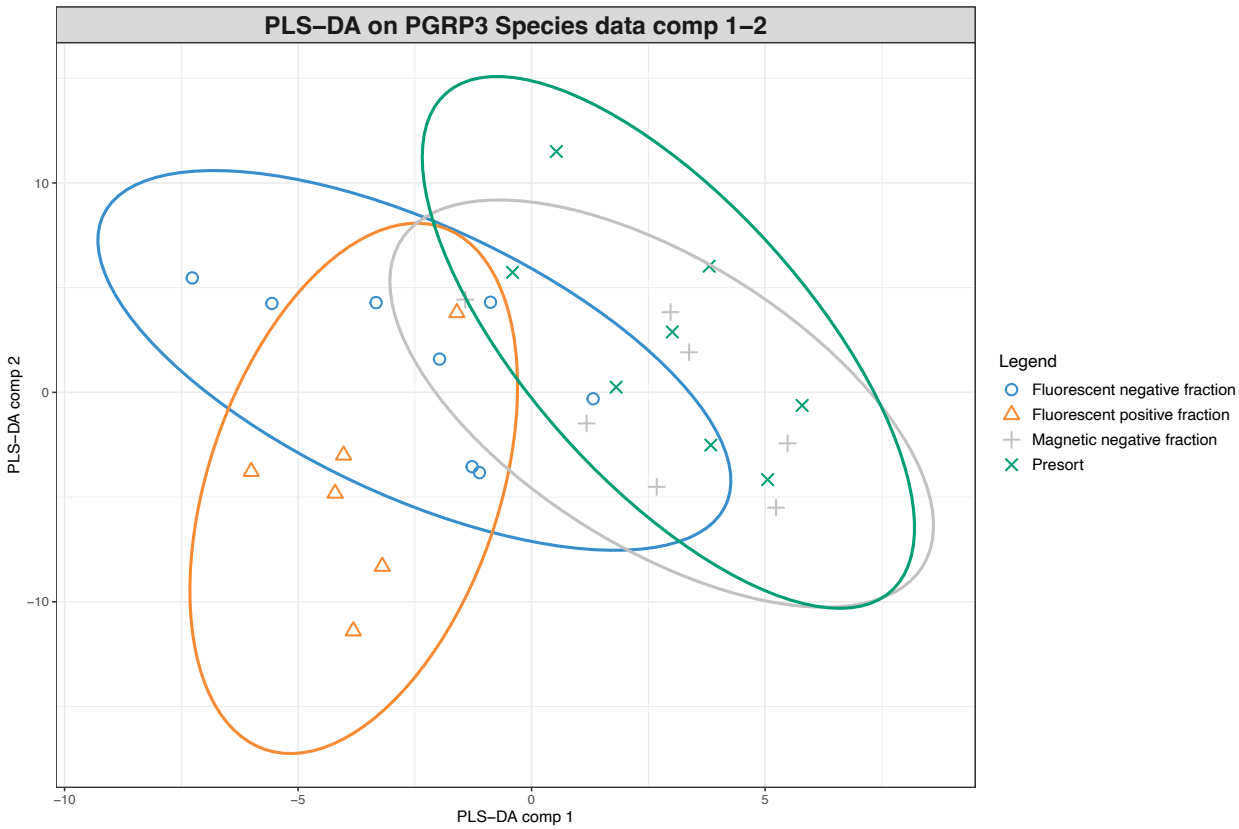

Figure 7 Heat map of top 50 microbial species featuring with significant differences compared to presort group in dental biofilm.
Row from left to right: fluorescence negative group, fluorescence positive group, magnetic negative group. Red: relative positive abundance of bacteria species compared to presort up to +20 times. Blue: relative negative abundance of bacteria species compared to presort up to -20 times.

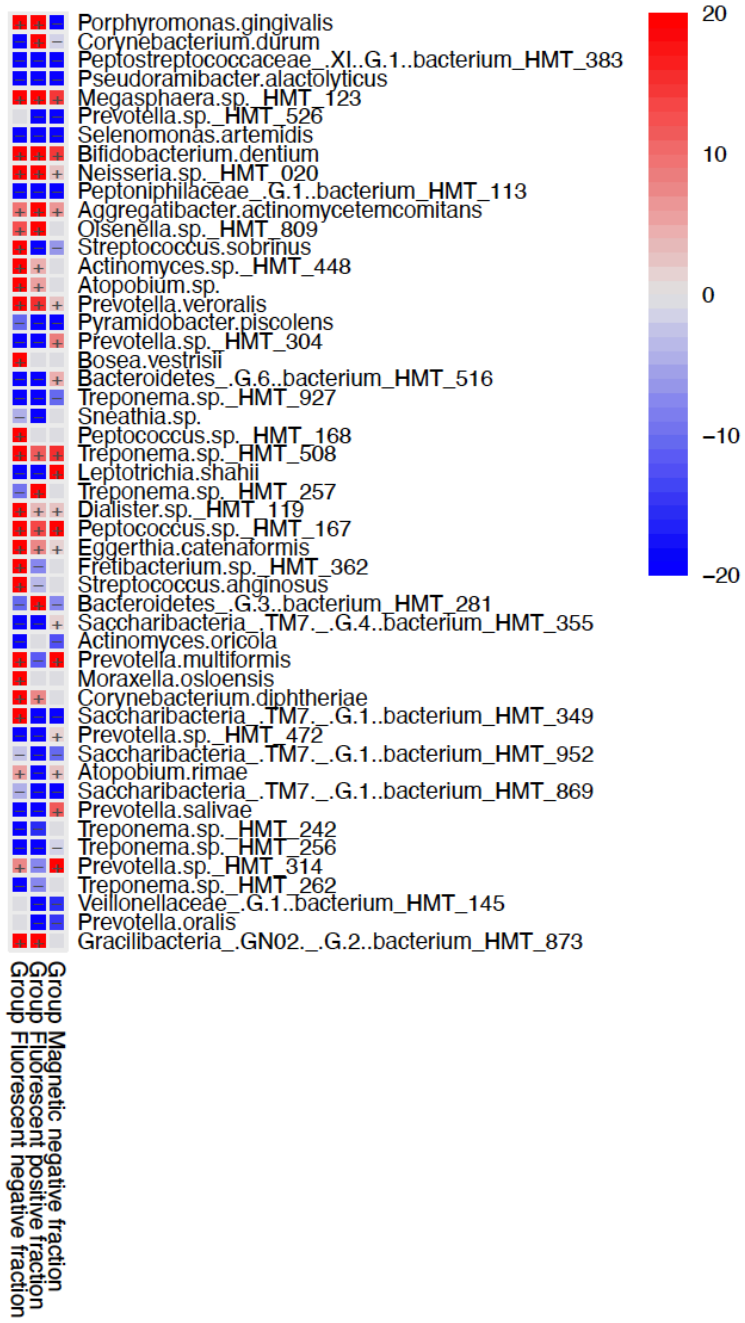

Figure 8 Relative abundance of representative PGRP3 highly coated bacteria in the different sort factions.

From left to right columns: presort group (blue), fluorescence negative fraction (red), fluorescence positive fraction (yellow), and magnetic negative fraction (green). This group of microbial species are selected as cell counts of fluorescence positive fraction (yellow) is significantly higher than presort (blue) and magnetic negative group (green)

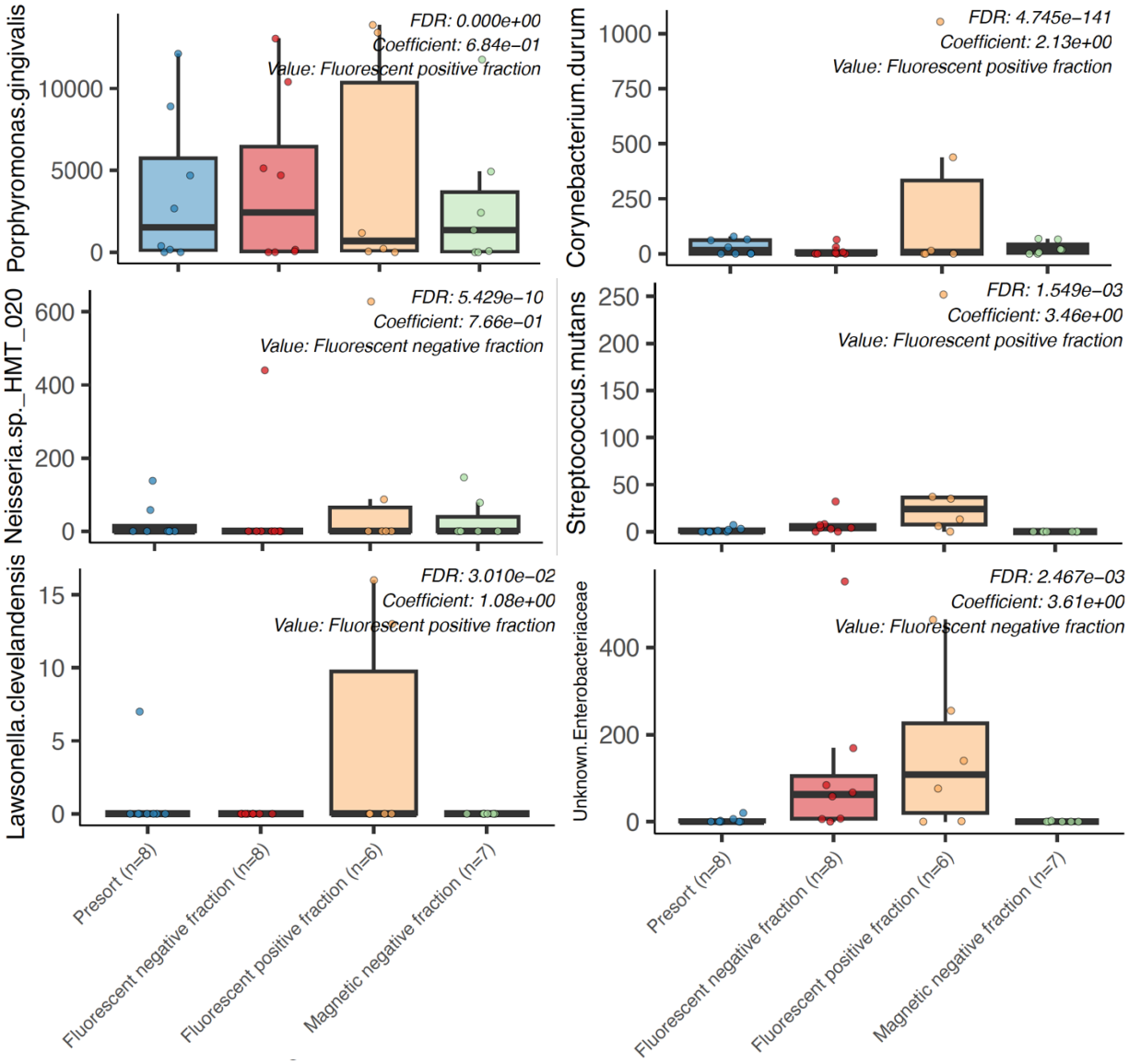

Figure 9 Relative abundance of representative bacteria that are not coated with PGRP3 in the different sort factions.
From left to right columns: presort group (blue), fluorescence negative fraction (red), fluorescence positive fraction (yellow), and magnetic negative fraction (green). This group of microbial species are selected as cell counts of fluorescence positive fraction (yellow) is significantly lower or minimal comparing to presort (blue) and magnetic negative group (green).

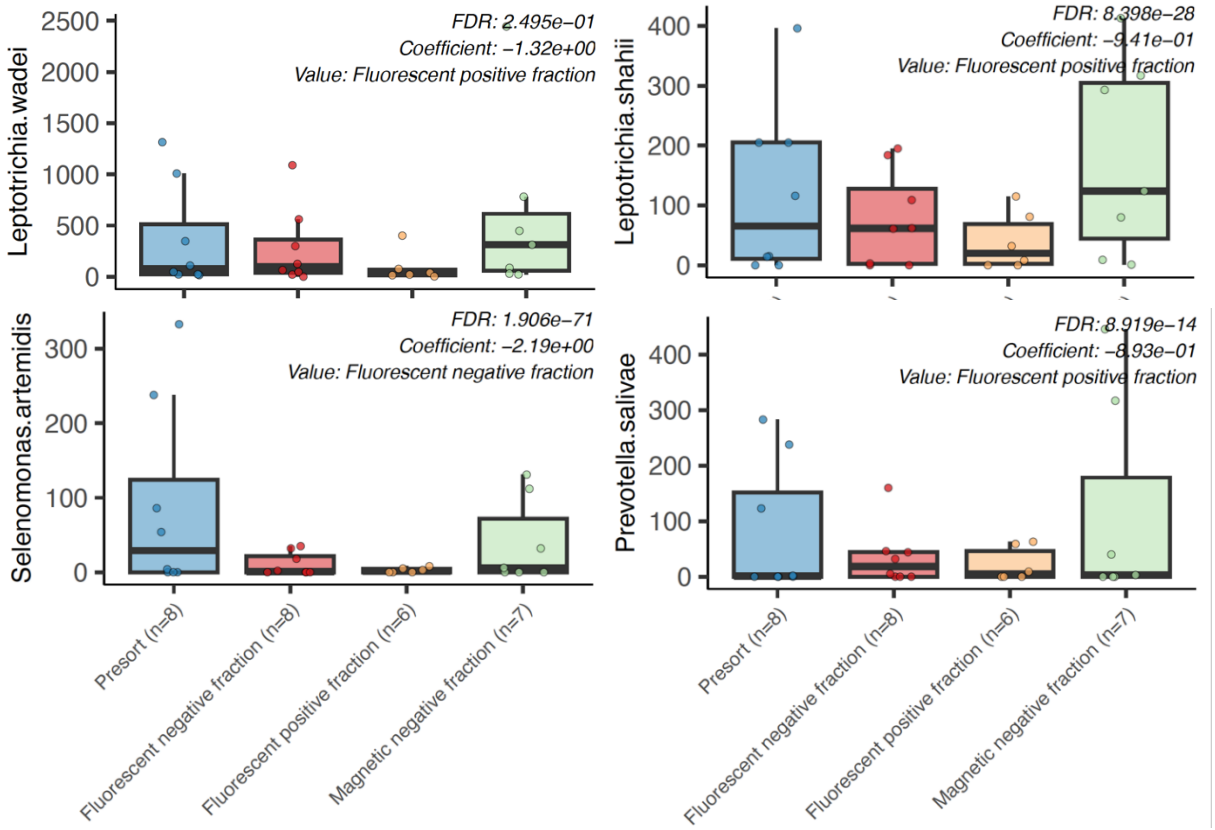

Figure 10: Relative abundance of three different unknown species of *Treponema. sp* in the different sort fractions.
From left to right columns: presort group (blue), fluorescence negative fraction (red), fluorescence positive fraction (yellow), and magnetic negative fraction (green). Top left: *Treponema.sp*._HMT_262; top right: *Treponema.sp*._HMT_927. Bottom left: *Treponema.sp*._HMT_257,

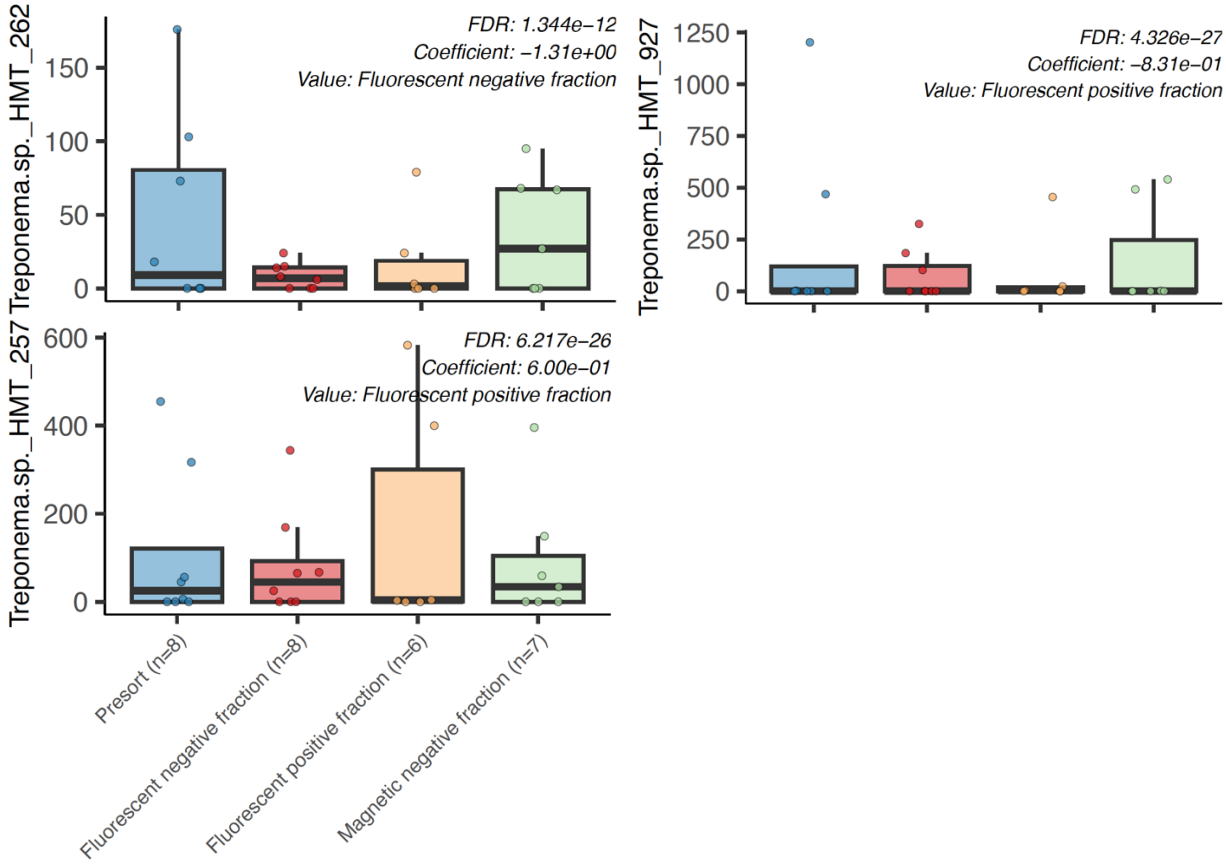

Table 1 Characteristics of the study population, comparing non periodontitis group (HG) and periodontitis group (PD)

	HG		PD			Total	
Variables	N or Mean	Percentage	N or Mean	Percentage	P value	N or Mean	Percentage
Subjects	4		8			12	100%
Age (years)	50.25		50.125		0.49	50.17	
Male	2	50.0%	5	62.5%	0.14	7	58%
Female	2	50.0%	3	37.5%	0.14	5	42%
Caucasian	3	75.0%	6	75.0%	0.23	9	75%
Other Ethnicity	1	25.0%	2	25.0%	0.23	3	25%
Diabetes	0	0%	0	0%		0	0%
Hypertension	0	0	1	12.50%		1	8%
			Periodontal Status				
	HG		**PD**			**Total**	
Periodontitis	0	0.0%	8	100.0%	<0.000001	8	66.67%
Stage III Grade B	0		6	75.0%	<0.000001	6	50.00%
Stage IV Grade C	0		2	25.0%	<0.000001	2	16.67%
Radiographic bone loss		2.50%		35%	0.002		24.17%
Probing Depth/PD (mm)	2.4		3.9		<0.000001	3.41	
Maximum PD(mm)	5		8.625		0.0011	7.42	
Bleeding on Probing (BOP)		6.11%		60.69%	0.00002		42.5025
Plaque Index (PI)		33.79%		94.02%	0.000002		73.94666667

Table 2 Summarized flow cytometry microbe counts and their percentages in total cell counts of magnetic positive fractions (PGRP3 coated microbes) for all subjects.
P1-P6: Periodontitis subjects; HG1, 4, 5: non periodontitis controls
FSC singles: isolated singlet cells
FITC+: cell counts of fluorescence positive fraction
FITC-: cell counts of fluorescence negative fraction

Subjects	FSC singlets	% total	FITC+	% parent	FITC -	% Parent
P1	175218	98.1	2412	1.4	160779	91.8
P2	17291	86.5	360	2.1	15891	91.9
P3	555767	55.5	9497	1.7	453514	81.6
P4	398097	39.8	2437	0.6	353192	88.7
P5	846619	84.7	193	0	833527	98.5
P6	1300792	79.2	6057	0.5	1234803	94.9
HG1	4357	91.8	0	0	4338	99.6
HG4	8283	84.9	5	0.1	7849	94.8
HG5	8558	88.7	5	0.1	8271	96.6

Appendix 1

AGE (PD vs HG)
t-Test: Two-Sample Assuming Unequal Variances

Age T test	*PD*	*HG*
Mean	50.125	50.25
Variance	212.98214	421.5833
Observations	8	4
Hypothesized Mean Difference	0	
df	5	
t Stat	-0.0108791	
P(T<=t) one-tail	0.4958703	
t Critical one-tail	2.0150484	
P(T<=t) two-tail	0.9917406	
t Critical two-tail	2.5705818	

Gender
t-Test: Paired Two Sample for Means

	HG	*PD*
Mean	2	4
Variance	0	2
Observations	2	2
Hypothesized Mean Difference	0	
df	1	
t Stat	-2	
P(T<=t) one-tail	0.147583618	
t Critical one-tail	6.313751515	
P(T<=t) two-tail	0.295167235	
t Critical two-tail	12.70620474	

Race
t-Test: Two-Sample Assuming Equal Variances

	HG	*PD*
Mean	2	4
Variance	2	8
Observations	2	2
Pooled Variance	5	
Hypothesized Mean Difference	0	
df	2	
t Stat	-0.89442719	
P(T<=t) one-tail	0.23273876	
t Critical one-tail	2.91998558	
P(T<=t) two-tail	0.46547752	
t Critical two-tail	4.30265273	

BONE LOSS
t-Test: Two-Sample Assuming Unequal Variances

	HG	*PD*
Mean	2.5	35
Variance	8.33333333	500
Observations	4	8
Hypothesized Mean Difference	0	
df	7	
t Stat	-4.04411161	
P(T<=t) one-tail	0.00245362	
t Critical one-tail	1.89457861	
P(T<=t) two-tail	0.00490725	
t Critical two-tail	2.36462425	

Mean Probing Depth (mm)
t-Test: Two-Sample Assuming Unequal Variances

	HG	*PD*
Mean	2.4	3.920625
Variance	0.143857143	0.717019583
Observations	8	16
Hypothesized Mean Difference	0	
df	22	
t Stat	-6.068154035	
P(T<=t) one-tail	2.0792E-06	
t Critical one-tail	1.717144374	
P(T<=t) two-tail	4.1584E-06	
t Critical two-tail	2.073873068	

Maximum Probing Depth (mm)
t-Test: Two-Sample Assuming Unequal Variances

	Variable 1	*Variable 2*
Mean	5	8.625
Variance	0.66666667	5.125
Observations	4	8
Hypothesized Mean Difference	0	
df	10	
t Stat	-4.03452839	
P(T<=t) one-tail	0.00119105	
t Critical one-tail	1.81246112	
P(T<=t) two-tail	0.00238209	
t Critical two-tail	2.22813885	

Gingivitis
t-Test: Two-Sample Assuming Unequal Variances

	PD	*HG*
Mean	1	0.75
Variance	0	0.25
Observations	8	4
Hypothesized Mean Difference	0	
df	3	
t Stat	1	
P(T<=t) one-tail	0.19550111	
t Critical one-tail	2.35336343	
P(T<=t) two-tail	0.39100222	
t Critical two-tail	3.18244631	

Plaque Index (PI %)
t-Test: Two-Sample Assuming Unequal Variances

	HG	*PD*
Mean	33.7975	94.0213
Variance	43.60069167	39.8647
Observations	4	8
Hypothesized Mean Difference	0	
df	6	
t Stat	-15.11116406	
P(T<=t) one-tail	2.64794E-06	
t Critical one-tail	1.943180281	
P(T<=t) two-tail	5.29588E-06	
t Critical two-tail	2.446911851	

Bleeing on Probing Index (BOP %)
t-Test: Two-Sample Assuming Unequal Variances

	HG	*PD*
Mean	6.115	60.69625
Variance	32.88136667	402.1491982
Observations	4	8
Hypothesized Mean Difference	0	
df	9	
t Stat	-7.136847407	
P(T<=t) one-tail	2.72185E-05	
t Critical one-tail	1.833112933	
P(T<=t) two-tail	5.4437E-05	
t Critical two-tail	2.262157163	

Reference

1. Socransky SS, Smith C, Haffajee AD. Subgingival microbial profiles in refractory periodontal disease. *Journal of clinical periodontology*. 2002;29(3):260-268.
2. Socransky SS, Haffajee AD. The nature of periodontal diseases. *Annals of periodontology*. 1997;2(1):3-10.
3. Deng Z-L, Szafrański SP, Jarek M, Bhuju S, Wagner-Döbler I. Dysbiosis in chronic periodontitis: key microbial players and interactions with the human host. *Scientific reports*. 2017;7(1):3703.
4. Abdulkareem AA, Al-Taweel FB, Al-Sharqi AJ, Gul SS, Sha A, Chapple IL. Current concepts in the pathogenesis of periodontitis: from symbiosis to dysbiosis. *Journal of Oral Microbiology*. 2023;15(1):2197779.
5. Dziarski R. Peptidoglycan recognition proteins (PGRPs). *Molecular immunology*. 2004;40(12):877-886.
6. Lu X, Wang M, Qi J, et al. Peptidoglycan recognition proteins are a new class of human bactericidal proteins. *Journal of Biological Chemistry*. 2006;281(9):5895-5907.
7. Zulfiqar F, Hozo I, Rangarajan S, Mariuzza RA, Dziarski R, Gupta D. Genetic association of peptidoglycan recognition protein variants with inflammatory bowel disease. *PLoS One*. 2013;8(6):e67393.
8. Saha S, Qi J, Wang S, et al. PGLYRP-2 and Nod2 are both required for peptidoglycan-induced arthritis and local inflammation. *Cell host & microbe*. 2009;5(2):137-150.
9. Baker BS, Powles A, Fry L. Peptidoglycan: a major aetiological factor for psoriasis? *Trends in immunology*. 2006;27(12):545-551.
10. Park SY, Gupta D, Kim CH, Dziarski R. Differential effects of peptidoglycan recognition proteins on experimental atopic and contact dermatitis mediated by Treg and Th17 cells. *PLoS One*. 2011;6(9):e24961.
11. Zenhom M, Hyder A, de Vrese M, Heller KJ, Roeder T, Schrezenmeir J. Peptidoglycan recognition protein 3 (PglyRP3) has an anti-inflammatory role in intestinal epithelial cells. *Immunobiology*. 2012;217(4):412-419.
12. Saha S, Jing X, Park SY, et al. Peptidoglycan recognition proteins protect mice from experimental colitis by promoting normal gut flora and preventing induction of interferon-γ. *Cell host & microbe*. 2010;8(2):147-162.
13. De Marzi MC, Todone M, Ganem MB, et al. Peptidoglycan recognition protein–peptidoglycan complexes increase monocyte/macrophage activation and enhance the inflammatory response. *Immunology*. 2015;145(3):429-442.
14. Kappeler S, Heuberger C, Farah Z, Puhan Z. Expression of the peptidoglycan recognition protein, PGRP, in the lactating mammary gland. *Journal of dairy science*. 2004;87(8):2660-2668.
15. Schmitz B, Radbruch A, Kümmel T, et al. Magnetic activated cell sorting (MACS)—a new immunomagnetic method for megakaryocytic cell isolation: comparison of different separation techniques. *European journal of haematology*. 1994;52(5):267-275.

16. Basu S, Campbell HM, Dittel BN, Ray A. Purification of specific cell population by fluorescence activated cell sorting (FACS). *Journal of visualized experiments: JoVE*. 2010(41).
17. O'Leary T. The periodontal screening examination. *The Journal of Periodontology*. 1967;38(6P2):617-624.
18. Miller SC. Textbook of Periodontia: oral medicine. *(No Title)*. 1943.
19. Carranza FA. *Glickman's clinical periodontology: prevention, diagnosis and treatment of periodontal disease in the practice of general dentistry*. Saunders; 1979.
20. Tonetti MS, Greenwell H, Kornman KS. Staging and grading of periodontitis: Framework and proposal of a new classification and case definition. *Journal of periodontology*. 2018;89:S159-S172.
21. Chapple IL, Mealey BL, Van Dyke TE, et al. Periodontal health and gingival diseases and conditions on an intact and a reduced periodontium: Consensus report of workgroup 1 of the 2017 World Workshop on the Classification of Periodontal and Peri-Implant Diseases and Conditions. *Journal of periodontology*. 2018;89:S74-S84.
22. NIH Human Microbiome Project - Core Microbiome Sampling Protocol A (HMP-A). https://www.ncbi.nlm.nih.gov/projects/gap/cgi-bin/study.cgi?study_id=phs000228.v4.p1. Published 2019. Accessed 2/13/19, 2019.
23. Sugiura K. A simple quantitative immunofluorescence assay for FITC-labeled antibody on platelets. *Journal of Immunological Methods*. 1981;40(2):165-170.
24. Shin J, Lee S, Go M-J, et al. Analysis of the mouse gut microbiome using full-length 16S rRNA amplicon sequencing. *Scientific reports*. 2016;6(1):29681.
25. Montassier E, Batard E, Massart S, et al. 16S rRNA gene pyrosequencing reveals shift in patient faecal microbiota during high-dose chemotherapy as conditioning regimen for bone marrow transplantation. *Microbial ecology*. 2014;67:690-699.
26. Rapin A, Pattaroni C, Marsland BJ, Harris NL. Microbiota analysis using an Illumina MiSeq platform to sequence 16S rRNA genes. *Current protocols in mouse biology*. 2017;7(2):100-129.
27. Ravi RK, Walton K, Khosroheidari M. MiSeq: a next generation sequencing platform for genomic analysis. *Disease gene identification: methods and protocols*. 2018:223-232.
28. Shahi SK, Zarei K, Guseva NV, Mangalam AK. Microbiota analysis using two-step PCR and next-generation 16S rRNA gene sequencing. *JoVE (Journal of Visualized Experiments)*. 2019(152):e59980.
29. Callahan BJ, McMurdie PJ, Rosen MJ, Han AW, Johnson AJA, Holmes SP. DADA2: High-resolution sample inference from Illumina amplicon data. *Nature methods*. 2016;13(7):581-583.
30. Caporaso JG, Kuczynski J, Stombaugh J, et al. QIIME allows analysis of high-throughput community sequencing data. *Nature methods*. 2010;7(5):335-336.
31. Bokulich NA, Kaehler BD, Rideout JR, et al. Optimizing taxonomic classification of marker-gene amplicon sequences with QIIME 2's q2-feature-classifier plugin. *Microbiome*. 2018;6:1-17.

32. Chen T, Yu W-H, Izard J, Baranova OV, Lakshmanan A, Dewhirst FE. The Human Oral Microbiome Database: a web accessible resource for investigating oral microbe taxonomic and genomic information. *Database*. 2010;2010.
33. Lee LC, Liong C-Y, Jemain AA. Partial least squares-discriminant analysis (PLS-DA) for classification of high-dimensional (HD) data: a review of contemporary practice strategies and knowledge gaps. *Analyst*. 2018;143(15):3526-3539.
34. Mallick H, Rahnavard A, McIver LJ, et al. Multivariable association discovery in population-scale meta-omics studies. *PLoS computational biology*. 2021;17(11):e1009442.
35. Dabdoub SM, Fellows ML, Paropkari AD, et al. PhyloToAST: Bioinformatics tools for species-level analysis and visualization of complex microbial datasets. *Scientific reports*. 2016;6(1):29123.
36. Chao A, Chiu C-H. Estimation of species richness and shared species richness. *Methods and applications of statistics in the atmospheric and earth sciences*. 2012:76-111.
37. Prakasam S, Merritt J, Kreth J. Pattern Recognition Beyond the Surface: Soluble Pattern Recognition and Their Role in Periodontitis. *Current oral health reports*. 2022;9(4):185-196.
38. Lin L-j, Lee C, Ranganathan S, Kreth J, Merritt J, Prakasam S. Identification of novel PGRP3 protein-protein interactions using yeast two hybrid system. *bioRxiv*. 2022:2022.2012. 2016.520769.
39. Olaso C-M, Viliunas J, McFall-Ngai M. A peptidoglycan-recognition protein orchestrates the first steps of symbiont recruitment in the squid-vibrio symbiosis. *Symbiosis*. 2022;87(1):31-43.
40. Swaminathan V, Prakasam S, Puri V, Srinivasan M. Role of salivary epithelial toll-like receptors 2 and 4 in modulating innate immune responses in chronic periodontitis. *Journal of periodontal research*. 2013;48(6):757-765.
41. Socransky S, Haffajee A, Cugini M, Smith C, Kent Jr R. Microbial complexes in subgingival plaque. *Journal of clinical periodontology*. 1998;25(2):134-144.
42. Listgarten M, Hellden L. Relative distribution of bacteria at clinically healthy and periodontally diseased sites in humans. *Journal of clinical periodontology*. 1978;5(2):115-132.
43. Datta H, Ng W, Walker J, Tuck S, Varanasi S. The cell biology of bone metabolism. *Journal of clinical pathology*. 2008;61(5):577-587.
44. Wolfgang WJ, Passaretti TV, Jose R, et al. Neisseria oralis sp. nov., isolated from healthy gingival plaque and clinical samples. *International journal of systematic and evolutionary microbiology*. 2013;63(Pt_4):1323-1328.
45. Treerat P, McGuire B, Palmer E, et al. Oral microbiome diversity: The curious case of Corynebacterium sp. isolation. *Molecular oral microbiology*. 2022;37(5):167-179.
46. Gupta D, States TToIUIU. Role of Bactericidal Peptidoglycan Recognition Proteins in Regulating Gut Microbiota and Obesity. 2018.
47. Zeng H, Chan Y, Gao W, Leung WK, Watt RM. Diversity of Treponema denticola and other oral treponeme lineages in subjects with periodontitis and gingivitis. *Microbiology spectrum*. 2021;9(2):e00701-00721.

48. Hu X, Shen X, Tian J. The effects of periodontitis associated microbiota on the development of oral squamous cell carcinoma. *Biochemical and Biophysical Research Communications*. 2021;576:80-85.
49. Colombo APV, Magalhães CB, Hartenbach FARR, do Souto RM, da Silva-Boghossian CM. Periodontal-disease-associated biofilm: A reservoir for pathogens of medical importance. *Microbial pathogenesis*. 2016;94:27-34.
50. da Silva-Boghossian CM, do Souto RM, Luiz RR, Colombo APV. Association of red complex, A. actinomycetemcomitans and non-oral bacteria with periodontal diseases. *Archives of oral biology*. 2011;56(9):899-906.
51. Theilade E. The non-specific theory in microbial etiology of inflammatory periodontal diseases. *Journal of clinical periodontology*. 1986;13(10):905-911.
52. Eke PI, Borgnakke WS, Genco RJ. Recent epidemiologic trends in periodontitis in the USA. *Periodontology 2000*. 2020;82(1):257-267.